

Automatic tracking for peritumoral fibers based on the Simple Harmonic Oscillator based Reconstruction and Estimation basis

Edward O. A. Konditty¹, Emmanuel Bonuedie¹, David Stern¹, and Alessandro Crimi^{1,2}

¹ African Institute for Mathematical Sciences, Ghana,
achola@aims.edu.gh,

² Swiss Federal Institute of Technology in Zurich (ETHZ), Switzerland
acrimi@vision.ee.ethz.ch

Abstract. Delineation of the Corticospinal tract is relevant in surgery for planning tumor resection or other types of treatments. To precisely delineate pathways within complex regions of white matter, it can be beneficial to use the information derived from high angular resolution diffusion imaging. In this manuscript we present the results of a deterministic approach on multi-shell diffusion data of magnetic resonance volume of patients with tumor. The implementation in Python extends the use of a library for tractography where an automatic region of interest delineation is also considered.

Keywords: Python, Tractography, SHORE basis, Tumor, Corticospinal tract, Dipy

1 Introduction

The Corticospinal Tract (CST) is a brain tract stemming from the motor cortex, passing through the Internal capsula and then through the cerebellar peduncle, and finally conducting impulses to the spinal cord. CST fulfills crucial roles in the organization of movements of the body, and damages to it cause spasticity and loss of ability to perform certain movements. The damages can be particularly pronounced in case of recurrent Glioma, Multiple Sclerosis and other types of injuries [1]. Moreover, brain lesions occurring in other parts of the brain can influence the CST by pushing its fibers. Tractography of CST is particularly challenging due to several fiber crossings and to several bifurcations where sub-fascicles are generated. For example the tracts for the face movements are often difficult to identify. Moreover, it has been reported that most of the lateral fibers of the CST are intractable using classical models such as diffusion tensors [2]. In this paper we investigate the usefulness of a Python implementation for multi-shell data tractography and automatic segmentation of the fibers in the CST.

2 Methods

In this section, we describe the probabilistic fiber tracking implemented in diffusion imaging in Python (Dipy) [3]. The pipeline comprises the estimation of the local diffusion model for each voxel, the definition of the seed points using a nonlinearly registered atlas and a deterministic tractography algorithm. This pipeline can be summarized in Fig 1.

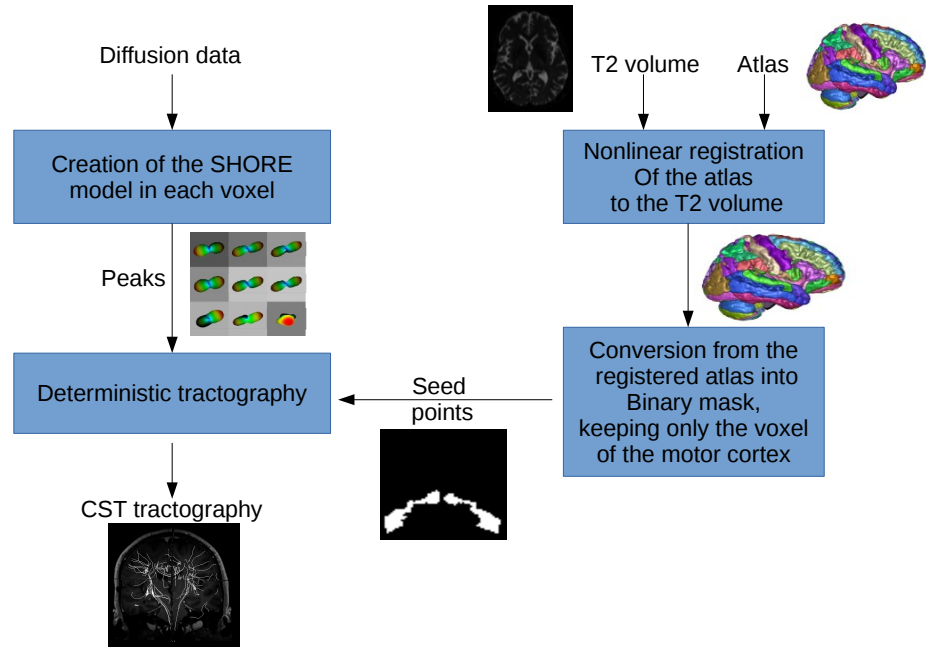


Fig. 1. Workflow diagram depicting the needed pipeline to obtain the CST tractography. Here the atlas is represented as the SRI24/TZO parcellation map [4], projected on cortical surface.

2.1 Diffusion Model

This paper adopts spherical harmonics (SH) representation based on constant solid angle (CSA) model. Diffusion Magnetic Resonance Imaging (MRI) aims at reconstructing the micro-structure of white matter by analyzing the diffusion weighted MRI (DWI) signals. The Ensemble Average Propagator (EAP) $E(q)$ describes the mean probability over the voxel of a displacement R in the effective diffusion time τ [5]. There are several methods to represent EAP. The Diffusion tensor model [6] considers the EAP as a Gaussian. This is however an over-simplification of the diffusion orientation of water molecules in the brain which

has a more complicated structure. Therefore, more advanced approaches have been proposed to go beyond this limitation such as the High Angular Resolution Diffusion Imaging (HARDI). Many measurements and a long acquisition time are necessary to obtain high-resolution EAP, to this end multiple-shells HARDI methods have been proposed. These methods aim at acquiring the signal following multiple shells schemes and then modeling it with adequate basis. Approaches for these circumstances are for instance Spherical Polar Fourier basis [7], Solid Harmonics [8], and the Simple Harmonic Oscillator based Reconstruction and Estimation (SHORE) method [9–11]. The SHORE basis was introduced by [9] using only orthogonal basis, while Cheng et al. [10] proposed a new formulation where the basis functions have an l_2 norm equal to one. The SHORE approach considers the diffusion signal attenuation $E(\mathbf{q})$ as given by the solution of the 3D quantum mechanical harmonic oscillator problem [9]:

$$E(\mathbf{q}) = \sum_{n=0}^N \sum_{l=0}^n \sum_{m=-l}^l c_{nlm} G_{nl}(q, \zeta) Y_l^m(u). \quad (1)$$

The radial part of SHORE basis with scale ζ is given by

$$G_{nl}(q, \zeta) = k_{nl}(\zeta) \left(\frac{q^2}{\zeta} \right)^{l/2} \exp \left(-\frac{q^2}{2\zeta} \right) L_{n-l/2}^{l+1/2} \frac{q^2}{\zeta}, \quad (2)$$

where $L_n^\alpha(x)$ is the generalized Laguerre polynomial, and $Y_l^m(\cdot)$ is a spherical harmonic function of degree l and order m , with

$$k_{nl}(\zeta) = \left[\frac{2}{\zeta^{3/2}} \frac{(n-l/2)!}{\Gamma(n+l/2+3/2)} \right]^{1/2}, \quad (3)$$

and where Γ is the Gamma function. The coefficients c_{nlm} can be obtained by convex quadratic optimization constrained by given condition such as that the probabilities are nonnegative over a large displacement space, and being the probabilities less than 1.

2.2 Region of Interest

Part of the proposed pipeline is the definition of the region of interest (ROI) from which the fibers stem have to be defined. To achieve the goal of segmenting peritumoral CST, ROIs need to be used. More specifically, the motor cortex of both brain hemispheres. Manual delineation of ROI is a tedious work and requires expertise. Moreover, other structures which are not the CST can be easily selected. Automatic delineation can be an advantage though it might be prone to error. In the proposed pipeline the necessary ROIs are obtained automatically using the indexed atlas SRI24 [4]. SRI24 is an MRI-based atlas of normal adult human brain anatomy, developed at the Stanford Research Institute (SRI), and generated by template-free nonrigid registration from images of 24 normal control subjects. The atlas is provided at 1mm isotropic image resolution and has

several regions of the brain marked using different intensity. This atlas is initially warped using diffeomorphic demon registration for elastic matching [12] to a T2 volume - which is considered the reference volume also for the diffusion data - and then only the voxels marked as representative for the motor cortex are kept and used as ROIs for the tractography part.

2.3 Euler method

Euler Delta Crossings [13] is a deterministic method for tractography [14, 15]. The streamlines are created from stemming seed points, which in our case are randomly selected from the external voxel of the ROIs of the prefrontal cortex. These seed points are the points from which the streamlines will start growing. Each seed point has initial coordinates (x, y, z) which can be defined as p_0 and is the beginning of the track propagation. Given such a point p_0 in a voxel, it is possible to solve a 3D path equation $\frac{ds(t)}{dt} = r(t)$, where $s(t)$ is the fiber curve path position at t and $r(t)$ is the local tangent direction of the path $s(t)$, this can be solved numerically by Euler’s method or higher order Runge-Kutta methods.

More specifically, the propagation is defined by solving the integration

$$p_t = p_0 + \int_0^t v(p(s))ds, \quad (4)$$

where Δs is the propagation step size, and v is the propagation direction. The next direction is defined by trilinear interpolation, by integrating directional information computed in the neighboring voxels. Stopping criteria are given by the value of a fractional anisotropy within a voxel which is below a defined threshold (in our case 0.02).

2.4 Data

The data are DWI scans acquired as multi-shells spine-echo EPI sequence with 4 different b-values: 200, 500, 1,000 and 3,000 s/mm², 69 diffusion-weighted volumes and 4 non-diffusion weighted volumes. The voxel size is 2.0 x 2.0 x 2.0 mm, 256 x 256 matrix for 73 slices. A T2 volume is used to register the data including the atlas. The volumes are from a patient with metastatic adenocarcinoma and a patient with a glioma in the middle of the left arcuate fasciculus.

3 Experiments

The model is instantiated with SHs of order 4 mapping on a sphere of 724 vertices, the minimum angular distance two peaks of the diffusion model was 25°, with the radial order of the SHORE basis of order 6 and $\zeta = 700$. Fig. 2 shows the overlay of the segmented CST and the original T1 volume.

Although the tumor delineation was not used in the algorithm, it can be seen in Fig. 2 that the CST in the right hemisphere is influenced by the presence of

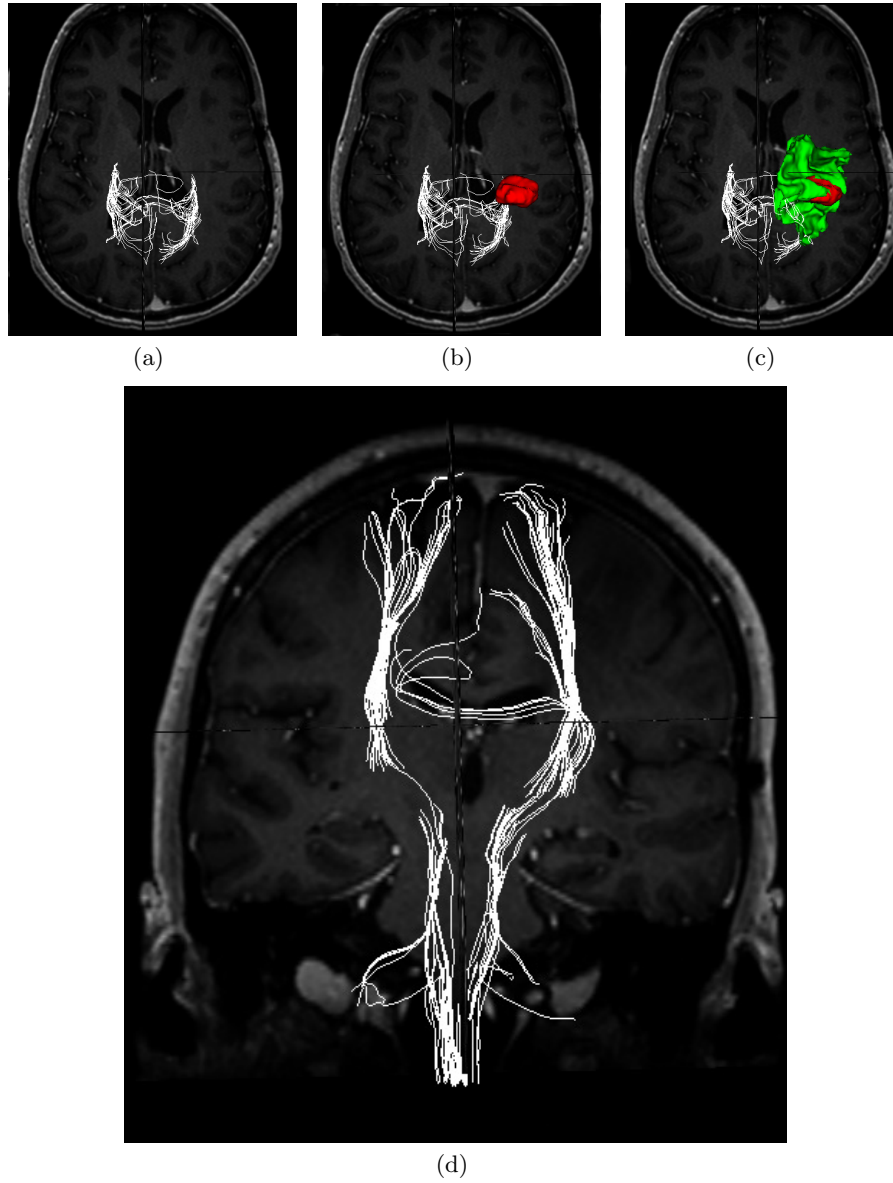


Fig. 2. Overlay of CST tractography, manually delineated structures and original T1 volume: (a) CST tracts, (b) CST and tumor segmentation, (c) CST and edema/tumor segmentation, (d) Coronal view of CST only, where some fibers on the left hemisphere are passing through the overlaid T1 slice and therefore are not so visible.

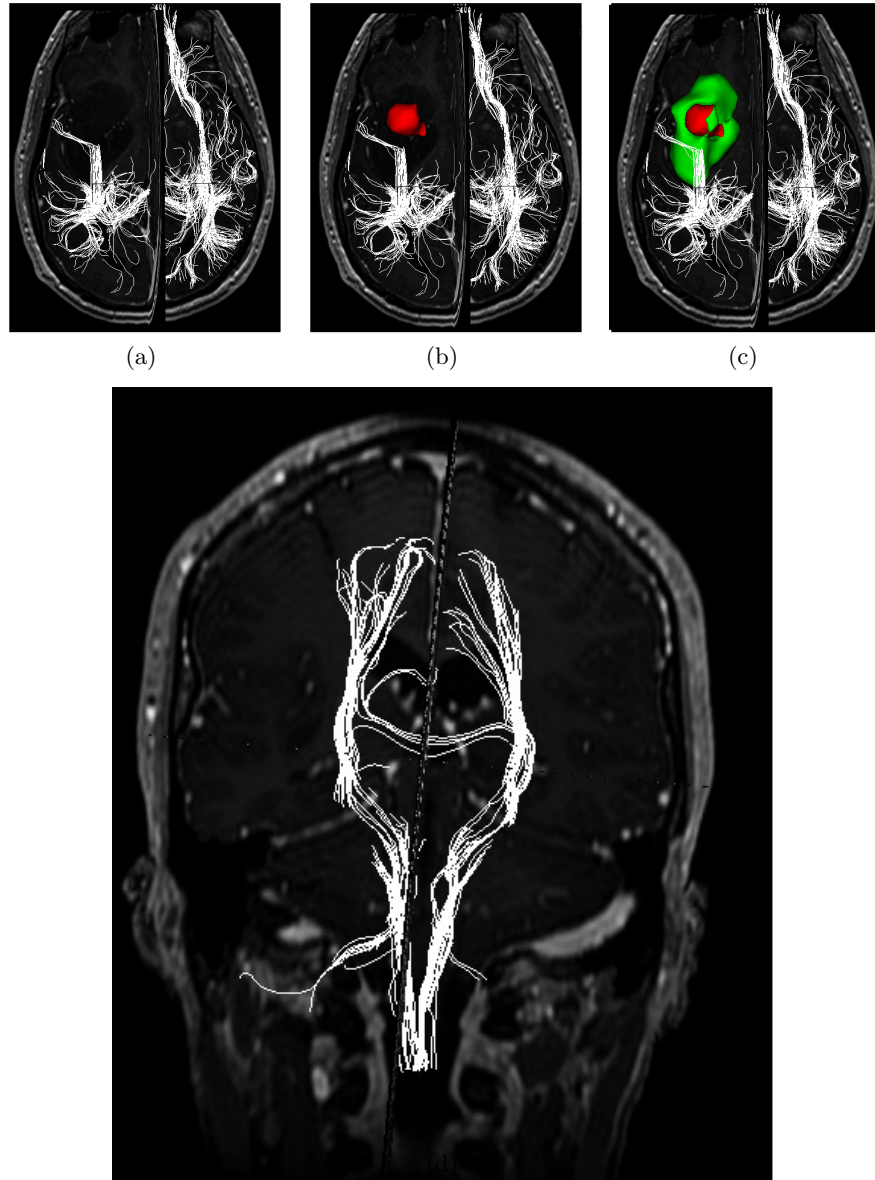


Fig. 3. Overlay of CST, arcuate fasciculus tractography, manually delineated structures and original T1 volume: (a) CST tracts and arcuate fasciculi, (b) CST, and arcuate fasciculi and tumor segmentation, (c) CST, and arcuate fasciculi and edema/tumor segmentation, (d) Coronal view of CST only.

the tumor. In fact some fibers in the right hemisphere seem pushed in caudal direction. Moreover, the edema is fully covering the tract of the right hemisphere.

For the patient with a glioma centered in the arcuate fasciculus in Fig. 3, the arcuate fasciculus in the left hemisphere appears interrupted/deflected, possibly disrupting the connection between the Broca’s and Wernicke’s area. To highlight the arcuate fasciculus the superior frontal gyri were given as ROIs for the seeding points, this introduced involuntarily also the tracking of the inferior longitudinal fasciculi since this fibers are also passing near the superior temporal gyrus. The inclusion of the inferior frontal gyrus as a further roi to track only the arcuate fasciculus is not advisable due to the presence of the glioma which might limit the connection of the two gyri. Tracts were saved using the Nibabel library [16] to be subsequently visualized with Trackvis [17] or eventually converted into vtk and visualized with MedINRIA [18].

4 Discussions and conclusion

The proposed method allows the visualization of the CST that can be used during tumor resection helping in preserving the motor functions. To use an automatic ROI segmentation has several advantages such as saving time from the tedious procedure of annotating the motor cortex and the possibility of scaling up the procedure and including easily other brain region annotated in the atlas. However, it cannot substitute the knowledge of a neurologist in this task, in fact it is believed to introduce some error (few fibers of the tapetum seem to be included). A probabilistic atlas with specific brain region could improve this aspect. Moreover, a qualitative study on the behavior of the different parameters and how these influence the tractography needs to be done, it has been carried out only empirically and qualitatively. The used data presented some challenges for example ringing effects were present in the diffusion volumes. To visualize the face tracts of the CST, it was necessary to increase the allowed angle within the Euler method to allow for 90 degrees turns and lower considerably the stopping threshold to less than 0.1, though these settings introduced further artifacts.

However, the approach can help surgery planning since it can highlight CST shifts due to tumors minimizing the possible handicap for the patient after surgery.

5 Acknowledgment

The authors would like to thank Dr. E. Garyfallidis for the useful advices and the effort on keeping alive the development of Dipy.

References

1. Q. Dong, R. C. Welsh, T. L. Chenevert, R. C. Carlos, P. Maly-Sundgren, D. M. Gomez-Hassan, and S. K. Mukherji, “Clinical applications of diffusion tensor imaging,” *Journal of Magnetic Resonance Imaging*, vol. 19, no. 1, pp. 6–18, 2004.

2. A. A. Qazi, A. Radmanesh, L. O'Donnell, G. Kindlmann, S. Peled, S. Whalen, C.-F. Westin, and A. J. Golby, "Resolving crossings in the corticospinal tract by two-tensor streamline tractography: Method and clinical assessment using fmri," *Neuroimage*, vol. 47, pp. T98–T106, 2009.
3. E. Garyfallidis, M. Brett, B. Amirbekian, A. Rokem, S. Van Der Walt, M. Descoteaux, I. Nimmo-Smith, and D. Contributors, "Dipy, a library for the analysis of diffusion mri data," *Frontiers in neuroinformatics*, vol. 8, 2014.
4. T. Rohlfing, N. M. Zahr, E. V. Sullivan, and A. Pfefferbaum, "The SRI24 multichannel atlas of normal adult human brain structure," *Human brain mapping*, vol. 31, no. 5, pp. 798–819, 2010.
5. P. T. Callaghan, *Principles of nuclear magnetic resonance microscopy*. Clarendon Press Oxford, 1991, vol. 3.
6. P. Basser, J. Mattiello, and D. LeBihan, "MR diffusion tensor spectroscopy and imaging," *Biophysical journal*, vol. 66, no. 1, pp. 259–267, 1994.
7. H.-E. Assemlal, D. Tschumperlé, and L. Brun, "Efficient and robust computation of pdf features from diffusion mr signal," *Medical image analysis*, vol. 13, no. 5, pp. 715–729, 2009.
8. M. Descoteaux, E. Angelino, S. Fitzgibbons, and R. Deriche, "Regularized, fast, and robust analytical q-ball imaging," *Magnetic Resonance in Medicine*, vol. 58, no. 3, pp. 497–510, 2007.
9. E. Ozarslan, C. Koay, T. Shepherd, S. Blackb, and P. Basser, "Simple harmonic oscillator based reconstruction and estimation for three-dimensional q-space mri," 2009.
10. J. Cheng, A. Ghosh, T. Jiang, and R. Deriche, "Model-free and analytical eap reconstruction via spherical polar fourier diffusion mri," in *Medical Image Computing and Computer-Assisted Intervention–MICCAI 2010*. Springer, 2010, pp. 590–597.
11. S. L. Merlet and R. Deriche, "Continuous diffusion signal, eap and odf estimation via compressive sensing in diffusion mri," *Medical image analysis*, vol. 17, no. 5, pp. 556–572, 2013.
12. T. Vercauteren, X. Pennec, A. Perchant, and N. Ayache, "Diffeomorphic demons: Efficient non-parametric image registration," *NeuroImage*, vol. 45, no. 1, pp. S61–S72, 2009.
13. E. Garyfallidis, "Towards an accurate brain tractography," Ph.D. dissertation, PhD thesis, University of Cambridge, 2012.
14. S. Mori, B. J. Crain, V. Chacko, and P. Van Zijl, "Three-dimensional tracking of axonal projections in the brain by magnetic resonance imaging," *Annals of neurology*, vol. 45, no. 2, pp. 265–269, 1999.
15. P. J. Basser, S. Pajevic, C. Pierpaoli, J. Duda, and A. Aldroubi, "In vivo fiber tractography using dt-mri data," *Magnetic resonance in medicine*, vol. 44, no. 4, pp. 625–632, 2000.
16. Nibabel. (2014) Nibabel, python library. [Online]. Available: <http://nipy.org/nibabel>
17. Trackvis. (2014) Trackvis, software page. [Online]. Available: <http://www.trackvis.org>
18. INRIA. (2014) Medinria, software page. [Online]. Available: <http://med.inria.fr/>